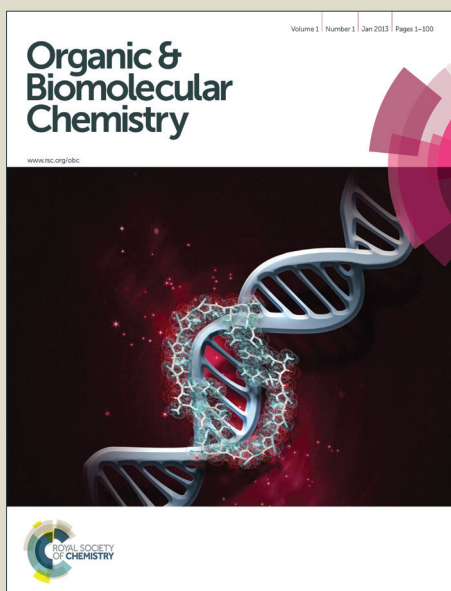


# Organic & Biomolecular Chemistry

Accepted Manuscript



This is an *Accepted Manuscript*, which has been through the Royal Society of Chemistry peer review process and has been accepted for publication.

*Accepted Manuscripts* are published online shortly after acceptance, before technical editing, formatting and proof reading. Using this free service, authors can make their results available to the community, in citable form, before we publish the edited article. We will replace this *Accepted Manuscript* with the edited and formatted *Advance Article* as soon as it is available.

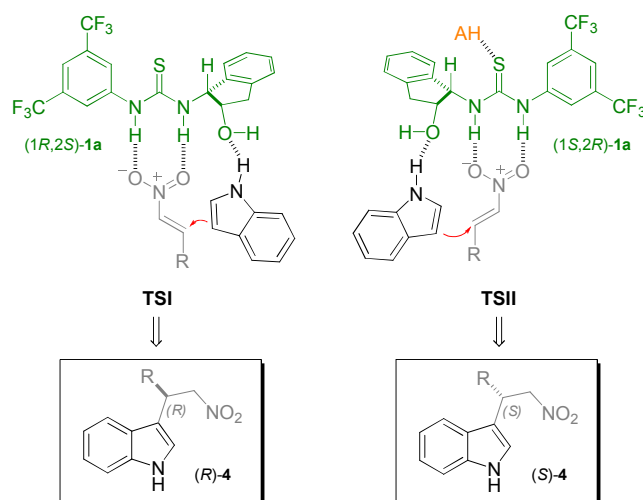
You can find more information about *Accepted Manuscripts* in the [Information for Authors](#).

Please note that technical editing may introduce minor changes to the text and/or graphics, which may alter content. The journal's standard [Terms & Conditions](#) and the [Ethical guidelines](#) still apply. In no event shall the Royal Society of Chemistry be held responsible for any errors or omissions in this *Accepted Manuscript* or any consequences arising from the use of any information it contains.

structure and the activation through hydrogen bonds of all species involved in the mechanism, which have been found to be crucial for the success of both reactions in terms of reactivity and enantioselectivity (TSIII, Figure 1).

presence of hydroxy group in the structure is important, it must be placed in the appropriate position, in order to efficiently drive the attack of the external nucleophile through hydrogen bonds coordination, as previously disclosed in Figure 1.<sup>5b,e,g</sup>

#### Previous work



#### Present work

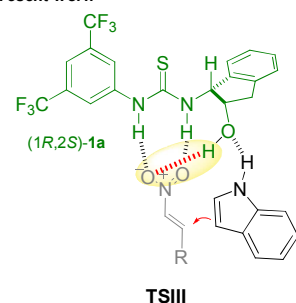
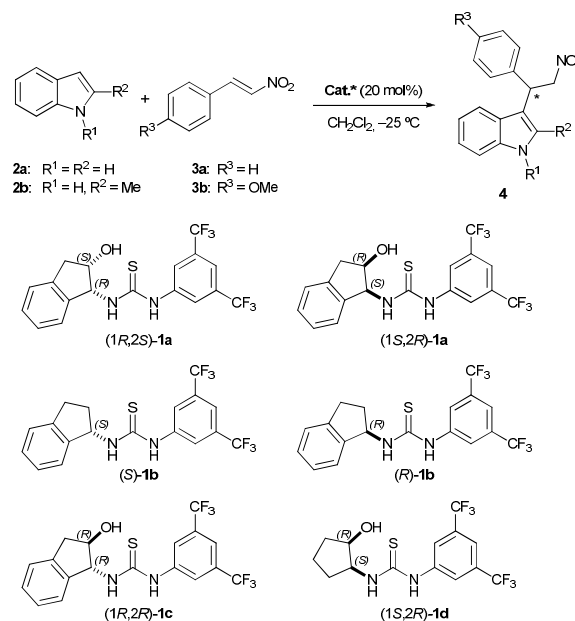


Fig. 1 Transition states proposed to explain the Friedel–Crafts alkylation reaction.

## Results and discussion

It has been accepted that the nucleophilic attack of the aromatic ring to the electrophile is the rate-determining step in the Friedel–Crafts reaction and the subsequent proton transfer is a faster process.<sup>12</sup> To evaluate our proposed mechanistic hypothesis we started the investigation studying computationally the C–C bond formation pathway, founded on experimental results (some of those experiments are compiled in Scheme 1 and Table 1). Although we observed already the importance of the hydroxy group in the structure of catalyst **1a** for the Friedel–Crafts alkylation reaction,<sup>5b,e,g</sup> we have recently realised about the importance of having the hydroxy group in the exact position in the catalyst skeleton. For example, we did not observe neither reactivity nor enantioselectivity with catalyst (1*R*,2*R*)-**1c**,<sup>5g</sup> with the hydroxy group in the *trans* position (Table 1, entries 6 and 7). This evidence supports that the hydroxy group must be in the skeleton in the *cis* configuration, playing a crucial role in the enantioselectivity and in the reactivity of the process. Therefore, even when the



Scheme 1 Thiourea catalysts tested in the Friedel–Crafts alkylation reaction.

Table 1. Thiourea-catalysed Friedel–Crafts alkylation reaction.<sup>a</sup>

Entry	Catalyst	Indole	T (°C)	time (h)	yield (%) <sup>b</sup>	ee (%) <sup>c</sup>
1 <sup>d</sup>	(1 <i>R</i> ,2 <i>S</i> )- <b>1a</b>	<b>2a</b>	−24	72	78	85 <sup>5b</sup> ( <i>R</i> )- <b>4aa</b>
2	(1 <i>S</i> ,2 <i>R</i> )- <b>1a</b>	<b>2a</b>	−25	72	40	82 <sup>5g</sup> ( <i>S</i> )- <b>4aa</b>
3 <sup>d</sup>	( <i>S</i> )- <b>1b</b>	<b>2a</b>	−24	72	15	Rac. <sup>f,5b</sup>
4 <sup>e</sup>	( <i>R</i> )- <b>1b</b>	<b>2a</b>	r.t.	120	24	Rac. <sup>f,5g</sup>
5	( <i>R</i> )- <b>1b</b>	<b>2a</b>	−25	72	n.d. <sup>g</sup>	Rac. <sup>f,5g</sup>
6	(1 <i>R</i> ,2 <i>R</i> )- <b>1c</b>	<b>2a</b>	r.t.	96	n.d. <sup>g</sup>	Rac. <sup>f,5g</sup>
7	(1 <i>R</i> ,2 <i>R</i> )- <b>1c</b>	<b>2a</b>	−25	120	n.d. <sup>g</sup>	10 ( <i>S</i> )- <b>4aa</b>
8	(1 <i>S</i> ,2 <i>R</i> )- <b>1d</b>	<b>2a</b>	−25	96	26	54 ( <i>S</i> )- <b>4aa</b>
9 <sup>d</sup>	(1 <i>R</i> ,2 <i>S</i> )- <b>1a</b>	<b>2b</b>	−45	72	82	74 <sup>5b</sup> <b>4ba</b>
10 <sup>e</sup>	(1 <i>S</i> ,2 <i>R</i> )- <b>1a</b>	<b>2b</b>	r.t.	72	94	20 <sup>5g</sup> <b>4ba</b>

<sup>a</sup> Experimental conditions: To a mixture of catalyst **1a–d** (20 mol%) and nitroalkene **3a** (0.1 mmol) in CH<sub>2</sub>Cl<sub>2</sub> (0.25 mL), indole **2a,b** (0.15 mmol) was further added, in a test tube at low temperature (−25 °C). After the reaction time, products **4** were isolated by flash chromatography. <sup>b</sup> Isolated yield. <sup>c</sup> Determined by chiral HPLC. <sup>d</sup> 0.1 mL CH<sub>2</sub>Cl<sub>2</sub>. <sup>e</sup> 0.5 mL CH<sub>2</sub>Cl<sub>2</sub>. <sup>f</sup> Racemic mixture. <sup>g</sup> Not determined.

In our mechanistic proposals (Figure 1), we hypothesised that the hydroxy group would drive the attack of the indole over a preferential face of the nitroalkene affording the desired product with the corresponding configuration depending on the enantiomer of the catalyst **1a** employed.<sup>5b,g</sup> The importance of the NH in the molecule of indole seems to be in concordance with a plausible hydrogen bond interaction with the OH of the catalyst (H-O...H-N), which would help in the orientation of the attack of the nucleophile. Remarkably, using catalysts **1b** and **1c** (Table 1, entries 3-7),<sup>5b,g</sup> the results are very poor in terms of both reactivity and selectivity. **TSI** and **TSII** could explain that in absence of the hydroxy group the reaction affords racemic mixture, since the indole could attack over both faces of the activated nitroolefin. However, they could not explain the lack of reactivity, which make us think that maybe the hydroxy group is involved in another crucial interaction, playing a dual mode of action (**TSIII**, Figure 1). On one hand, it would drive the attack of the indole over the nitroalkene as conductor, and on the other hand, it should be also involved in the activation of the nitroalkene. In this sense, the OH could govern the reactivity of the process explaining the lack of reactivity in the absence of it. These experimental observations encouraged us to deeply study, by the first time, the proposed dual role of the hydroxy group in the transition state and to elucidate the mechanism of this Friedel–Crafts alkylation reaction using catalyst **1a**.<sup>13</sup>

#### Theoretical calculations based on the real catalytic system

All the calculations were carried out at the PCM(CH<sub>2</sub>Cl<sub>2</sub>)/M06-2X/6-311G(d,p) level,<sup>14</sup> including minima, transition states, structure optimisations and frequencies analyses. The thermal and entropic contributions to the free energies were also obtained from the vibrational frequencies analyses, performed at -24 °C, which is the temperature at which the highest experimental enantiomeric excess was obtained. Although the mechanism of our reaction was studied at the beginning in a simplified system, for more clarity we report here only the complete system with catalyst (1*R*,2*S*)-**1a**, indole (**2a**) and nitrostyrene (**3a**), in order to obtain a more accurate approach of our active system in the rate determining step.

To proof the robustness of our mechanism different parameters have been widely analysed. In this sense, the conformations of the catalysts, the attack through both faces of the nitroalkene, the possibility of bidentate or monodentate coordination through directional hydrogen bonds between the

nitroalkene and the thiourea, the coordination of the hydroxy group to the indole and the approaching face of the indole, have been some key aspects of this comprehensive study. In order to test the accuracy of our proposed mechanism we analysed different transition states for the C-C bond formation step, that is the attack of indole **2** over the nitroalkene **3** activated with thiourea catalyst (1*R*,2*S*)-**1a** through hydrogen bond interactions, using the complete catalytic system. The analysis of the global reactivity in terms of Fukui's indices for indole **2**, the nitroalkene **3** and the active catalytic complex have been also calculated at the ground state (see supporting information).

In this respect, we have focused this computational work on the study of all possible hydrogen bond interactions between all involved species what is expected to stabilize the catalytic system in the transition state. Based on an extensive conformational search, we were able to find several transition states. Among all possibilities studied, only the most stable transition states calculated are represented in Figure 2, in which the reaction occurs through a concomitant coordination of both reagents. Additionally, in these transition states some relevant distances have been pointed out, indicating the formation of a C-C bond or all plausible hydrogen bond interactions involved in the process activation. These values are related with the interactions between the NH of the thiourea **1** and the nitroalkene **3**, the C-C bond formation between the indole **2** and the nitroalkene **3**, the coordination between the OH of the catalyst **1** and the NH of indole **2**, and even more interesting is the interaction found for the hydroxy group and one of the oxygen atoms of the nitroalkene **3** (O-H...O-N=O) (**TS1**, **TS2**, **TS5** and **TS6**). Furthermore, a relevant additional interaction has been also found between the H atom of the hydroxy group and the S atom of the thiourea (O-H...S), acting as hydrogen acceptor (**TS3** and **TS4**).

We have also examined the energetic cost for the uncatalysed reaction represented in Scheme 1, between indole (**2a**) and nitrostyrene (**3a**), and that it is 28 kcal/mol, in contrast to 11 kcal/mol for  $\Delta G^\ddagger$  in the case of **TS1**, the most stable one for the catalysed reaction (Figure 2). This outcome is consistent with the stabilizing effect promoted by the presence of the catalyst and the subsequent acceleration of the reaction. Free energy values for the calculated transition states are relative to the most stable **TS1**, to which was assigned value 0 of energy.

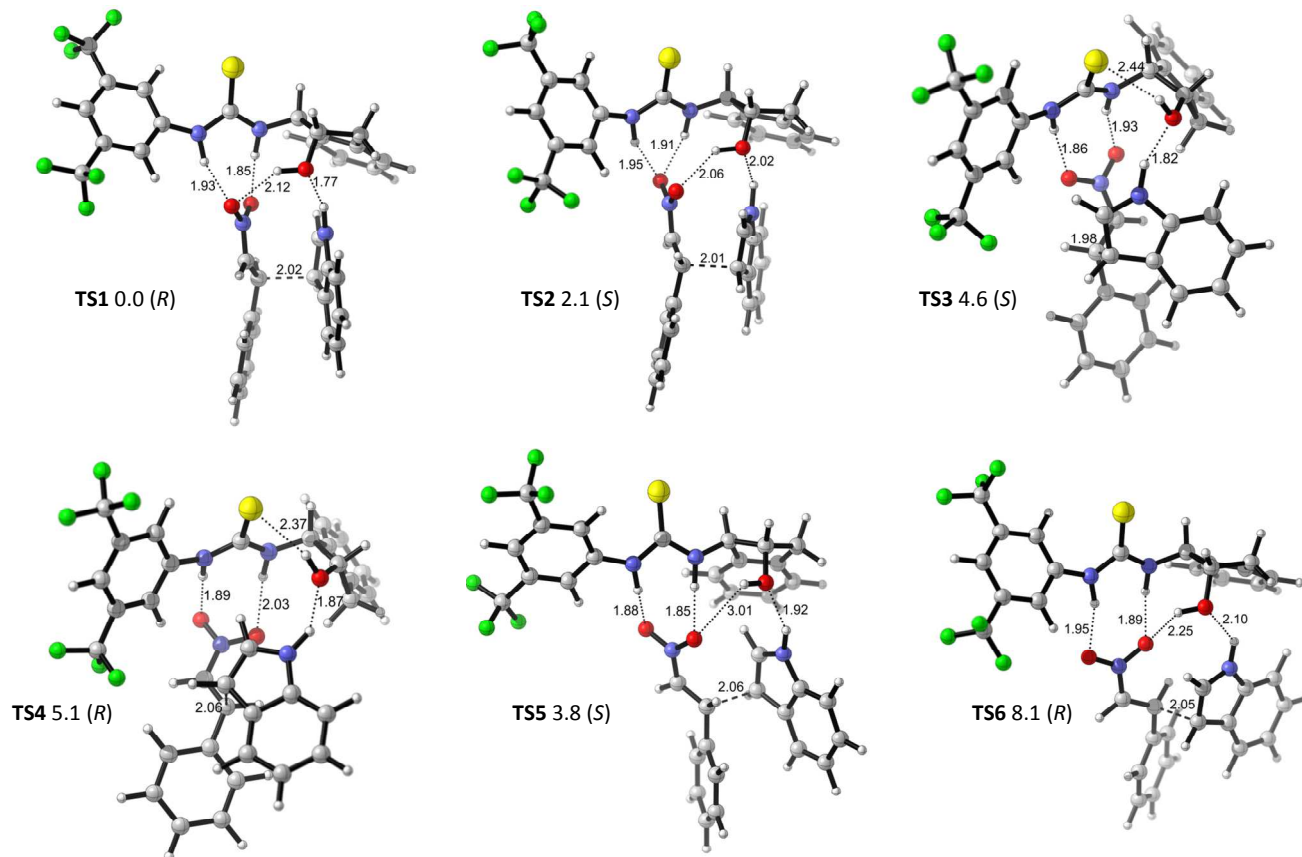


Fig. 2 Transition states for the Friedel–Crafts alkylation reaction. Relative free energies expressed in kcal/mol; distances in Å.

Some interesting conclusions could be extracted from these outcomes (Figure 2). In all cases, the oxygen atom of the hydroxy group of the catalyst **1a** prefers to interact with the NH of the indole (**2a**) through H–O...H–N, leading to the attack of the nucleophile over the nitroalkene **3**, as we previously predicted (Figure 1).<sup>5b,g</sup> The small differences in activation barriers between the attack of indole (**2a**) over the *Si* face of the nitrostyrene (**3a**) (**TS1**, 0.0 kcal/mol) and the *Re* face (**TS2**, 2.1 kcal/mol) could justify that the higher enantiomeric excess achieved was around 85% (Table 1, entries 1 and 2). According to the experiments, the most stable transition state **TS1** would afford the *R* enantiomer of the final product (*R*)-**4aa** obtained with (1*R*,2*S*)-**1a** (Table 1, entry 1).<sup>5b</sup> The opposite is true for the catalyst (1*S*,2*R*)-**1a**, which would afford the *S* enantiomer of **4** (Table 1, entry 2). To unambiguously establish the absolute configuration of the final Friedel–Crafts adducts **4** using catalyst (1*S*,2*R*)-**1a**, single crystal was grown from adduct **4ab**.

As expected, the stereochemical outcome was determined to be *S* for final product **4** (Figure 3).<sup>15</sup>

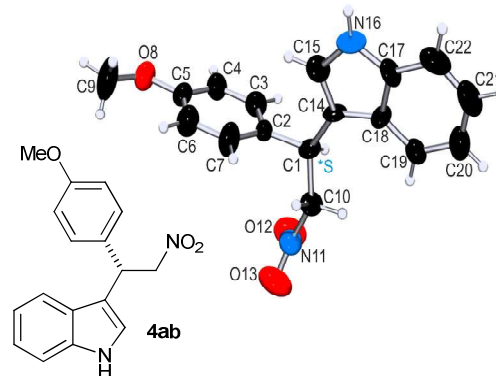


Fig. 3 X-Ray crystal structure of (*S*)-**4ab**.

Moreover, it is interesting to note that except in **TS2**, the nitroalkene **3** prefers to be coordinated through a bidentate coordination, as pioneering observed by Etter and co-workers.<sup>16</sup> This bidentate coordination provides a more rigid TS among the three species, although previous works have also postulated a plausible monodentate coordination between a thiourea and a nitroalkene.<sup>17</sup> The stability of the more stable transition state **TS1** could be attributed to a less hindered packaging, since the indole (**2a**) is farther from the aromatic ring of the aminoindanol part of the catalyst than in **TS2**, which would cause stronger repulsions. In this sense, the indole–nitroalkene relative orientation plays a crucial role determining the selectivity observed in final products **4**.

Having identified the most stable transition state **TS1**, we proceeded to firstly vary the structure of the catalyst **1** and then the indole **2**. Centred on our experiments, we examined the TS for catalyst (*S*)-**1b** (Figure 4). The outcome of replacing the OH by H in the catalyst was interesting. First of all, the energetic differences among the different conformations of the catalytic system affording enantiomers (*R*)-**4** and (*S*)-**4**, are reduced. This trend supports the observed racemic mixture when catalyst **1b** is used (Table 1, entries 3-5).

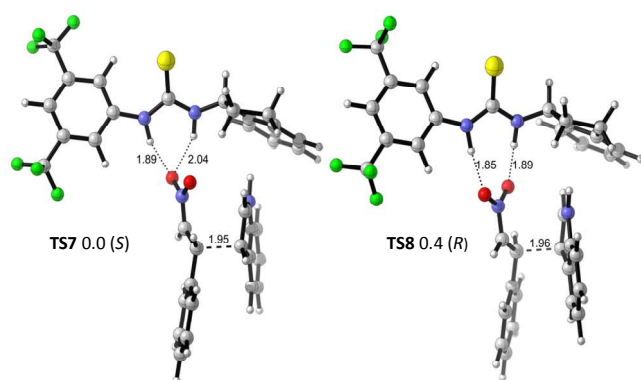


Fig. 4 Transition states for the Friedel–Crafts alkylation reaction using catalyst (*S*)-**1b**. Relative free energies expressed in kcal/mol; distances in Å.

$\Delta G^\ddagger$  for **TS7** was found to be 17 kcal/mol, 6 kcal/mol more energetic than in the case of **TS1**, which demonstrates that the hydroxy group has not only a driving effect in this process, orientating the attack of the indole **2**, but also a stabilising effect. This is also in concordance with the experimental outcomes reached, since the reaction proceeds scarcely and in a racemic way (Table 1, entries 3-5).

A similar effect is observed when catalyst (*1R,2R*)-**1c** is employed, which has a *trans* configuration (Figure 5). Interestingly, in this case a preferred hydrogen bond interaction between the hydroxy group and the S atom of the thiourea is found (O–H...S). This coordination does not stabilise the TS more than in the absence of the hydroxy group, since the  $\Delta G^\ddagger$  for **TS9** was found to be 18 kcal/mol, the same order of energy than that obtained in **TS7** (17 kcal/mol). In both reactions, the high  $\Delta G^\ddagger$  values fit with the almost lack of reactivity observed (Table 1, entries 6 and 7).

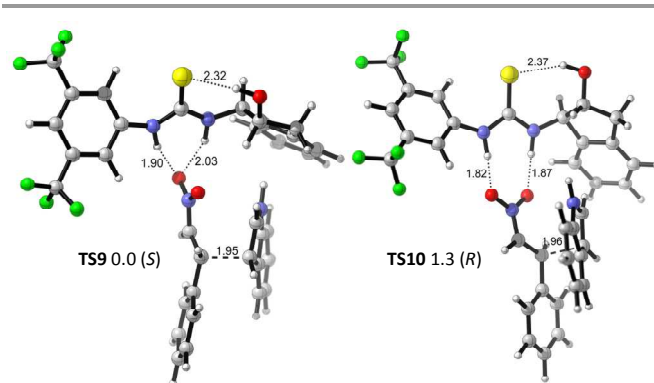


Fig. 5 Transition states for the Friedel–Crafts alkylation reaction using catalyst (*1R,2R*)-**1c**. Relative free energies expressed in kcal/mol; distances in Å.

In this case, the obtainment of the same enantiomer (*R*)-**4aa** would be expected, since the configuration of the carbon bearing the NH group in the aminoindanol structure of the catalyst is the same as in catalyst (*1R,2S*)-**1a** (Table 1, entry 1). Remarkably, a variation in the final enantiomer is computationally predicted because the attack of the indole **2** occurs preferentially by the *Re* face of the nitroalkene **3**, affording *S* configuration in the final product **4**. This result is in accordance with the experimental outcome (Table 1, entry 7). Although the energetic differences between both transition states (**TS9** and **TS10**) are small, the preferred *S* configuration could be due a more congestive conformation in **TS10** between the indole **2** and the aminoindanol ring of the catalyst. In this case, we found preferential monodentate coordination between the nitrostyrene (**3a**) and the thiourea (*1R,2R*)-**1c** (**TS9**).

Furthermore, we analysed the effect of the catalyst in the absence of the aromatic ring in the aminoindanol skeleton, that is, using (*1R,2S*)-**1d** (Figure 6). The most stable transition states (**TS11** and **TS12**) are similar to **TS1** and **TS2**, even with the same differences in energy and with the same favoured coordination by the hydroxy group to the NH in the indole **2** (H–O...H–N) and to the O atom in the nitro group of the alkene **3** (O–H...O–N=O).  $\Delta G^\ddagger$  for **TS11** was found to be 12.5 kcal/mol, 1.5 kcal/mol more energetic than in the case of **TS1**. Although, the absence of the aromatic ring seems not to have great effects in the calculated energies, the experimental results are really different to those reached with catalyst **1a** (Table 1, entries 1, 2 and 8). In this case, the influence of the aromatic ring seems to be really important in the origin of the selectivity of the process. We can envision a strong steric effect of the aromatic ring in catalyst **1a**, avoiding the attack of the indole **2** by the other side, that in the case of catalyst **1d** does not exist.

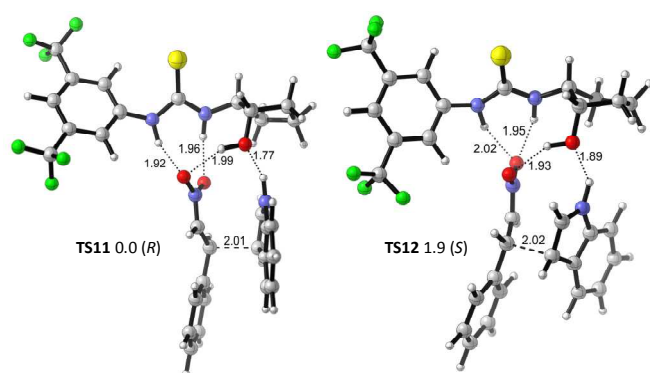


Fig. 6 Transition states for the Friedel–Crafts alkylation reaction using catalyst (1*R*,2*S*)-**1d**. Relative free energies expressed in kcal/mol; distances in Å.

After analysing the catalyst structure, we further considered varying the indole skeleton (Figure 7). When we explored 2-methylindole (**2b**) as nucleophile, the central core of the most stable transition states and all the hydrogen bonds remain unaltered compared with **TS1** and **TS2** (Figure 2). However, the difference in energy between both **TS13** and **TS14** is very weak. The  $\Delta G$  is in agreement with the less enantioselective process observed (Table 1, entries 9 and 10).  $\Delta G^\ddagger$  for **TS13** was found to be 9.0 kcal/mol. The energy barrier is much lower (2.1 kcal/mol) than in the case of **TS1**, indicating much higher reactivity. This behaviour agrees well with the higher reaction rate observed in this process, due to the inductive effect provided by the methyl group, which favours the attack through the third position of the indole **2b**.

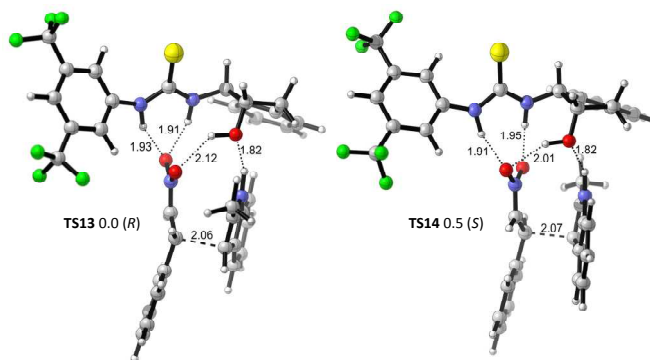


Fig. 7 Transition states for the Friedel–Crafts alkylation reaction of **2b** using catalyst (1*R*,2*S*)-**1a**. Relative energies expressed in kcal/mol; distances in Å.

It is worth noting that we found a preferred monodentate coordination between the thiourea and the nitroalkene **3** (**TS13**). The coordination of the hydroxy group to the nitro group through O–H...O–N=O is also found in both transition states (**TS13** and **TS14**, Figure 7).

With all these outcomes in mind we are pleased to slightly modify our previous two transition states **TSI** and **TSII** (Figure 1), which were not far from the possible mechanistic activation. In order to better understand the experimental results, we include now the crucial interaction between the OH group of the catalyst and an oxygen atom of the nitroalkene (O–H...O–

N=O) (Figure 1, **TSIII**). These theoretical calculations have underlined the essential role of the hydrogen bonding in the success of the process.

## Conclusions

We have reported an unprecedented theoretical study of the mechanism of thiourea-catalysed Friedel–Crafts alkylation reaction for the addition of indoles **2** to nitroalkenes **3**. The catalyst centre of study was the aminoindanol derived thiourea (1*R*,2*S*)-**1a** and its enantiomer (1*S*,2*R*)-**1a**. Some other catalysts derived from this crucial structure have been also considered. Our work sheds light on the experimental results obtained in this process and supports them. Additionally, the computational results are according to our previous disclosed mechanisms (Figure 1).

It is revealed that indole **2** is coordinated to the crucial hydroxy group of the catalyst through a hydrogen bond (HO...H–N) and the nitroalkene **3** is preferentially coordinated via bidentate hydrogen bonds with the thiourea **1**. Additionally, we have found an interesting interaction between the hydroxy group of the catalyst **1** and an oxygen atom of the nitro group of the nitroalkene **3** (O–H...O–N=O), supporting the lack of reactivity when the OH function is not present in the catalyst structure. Based on extensive computational studies, we can elucidate the preference in the attack of the indole **2** over the appropriate face of the nitroalkene **3** affording the observed major enantiomer in each case. This clarifies the origin of the enantioselectivity in this Friedel–Crafts alkylation reaction for different catalyst structures and indoles. We think that our work could be an important theoretical study to explain the role of the aminoindanol skeleton in organocatalysts, specially the role of the hydroxy group, and it could help to understand future mechanisms where the aminoindanol structure is involved.

## Experimental Section

**Materials.** All commercially available solvents and reagents were used as received. CH<sub>2</sub>Cl<sub>2</sub> was filtered through basic alumina prior to use to avoid the presence of trace amounts of acid. The <sup>1</sup>H and <sup>13</sup>C NMR spectra for catalysts (1*R*,2*S*)-**1a**,<sup>5b</sup> (1*S*,2*R*)-**1a**,<sup>5g</sup> (*S*)-**1b**,<sup>18</sup> (*R*)-**1b**,<sup>5g</sup> (1*R*,2*R*)-**1c**,<sup>5g</sup> and (1*S*,2*R*)-**1d**,<sup>5e</sup> and final products **4aa**,<sup>5g</sup> **4ab**<sup>5g</sup> and **4ba**<sup>5g</sup> are consistent with values previously reported in the literature.

## Representative procedure for thiourea organocatalysed Friedel–Crafts alkylation reaction of indole with nitroalkenes.

To a mixture of catalyst **1a-d** (20 mol%) and nitroalkene **3a** (0.1 mmol) in CH<sub>2</sub>Cl<sub>2</sub> (0.1, 0.25 or 0.5 mL), indole **2a,b** (0.15 mmol) was further added, in a test tube at low temperature (–25 °C). After the appropriate reaction time (see Table 2), the residue was purified by flash chromatography (SiO<sub>2</sub>; hexane/EtOAc, 8:2) to afford final adducts **4**. Yields and enantioselectivities are reported in Table 2. Spectral and

analytical data for compounds **4** are in agreement with those previously reported in the literature.<sup>5g</sup>

**Computational Methods.** All the calculations were performed using the Gaussian09 program.<sup>14</sup> Molecular geometries were optimized with the M06-2X functional<sup>19</sup> in conjunction with the 6-311G(d,p) basis set.<sup>20</sup> Analytical second derivatives of the energy were calculated to classify the nature of every stationary point, to determine the harmonic vibrational frequencies, and to provide zero-point vibrational energy corrections. The thermal and entropic contributions to the free energies were also obtained from the vibrational frequency calculations, using the unscaled frequencies, and a value of -24°C for the temperature (because that is the temperature at which the highest experimental enantiomeric excess was obtained). Full optimization calculations have been carried out considering solvent effects (CH<sub>2</sub>Cl<sub>2</sub>) with the PCM model.<sup>21</sup>

### Acknowledgements

We thank the Spanish Ministry of Economía y Competitividad (MICINN, Madrid, Spain. Project CTQ2010-19606) and the Government of Aragón (Zaragoza, Spain. Research Group E-10) for financial support of our research. D.R.-L. thanks the Spanish Ministry of Education (MEC) for a pre-doctoral grant (FPU program). We thank Dr. Pablo J. Sanz Miguel (ISQCH) for X-ray structure analysis. We acknowledge the Institute of Biocomputation and Physics of Complex Systems (BIFI) at the University of Zaragoza for computer time at clusters Terminus and Memento. Molecular graphics have been performed with CYLview 1.0 software (C. Y. Legault, University of Sherbrooke, Canada).

### Notes and references

<sup>a</sup> Laboratorio de Síntesis Asimétrica, Departamento de Química Orgánica. Instituto de Síntesis Química y Catálisis Homogénea (ISQCH). CSIC-Universidad de Zaragoza. E-50009 Zaragoza, Aragón, Spain Phone: +34 976761190. E-mail: raquelph@unizar.es Electronic Supplementary Information (ESI) available: CCDC-976490. Absolute (hartrees) and relative (kcal mol<sup>-1</sup>) electronic and free energies calculated at -24 °C, including Cartesian coordinates of optimized structures at PCM(CH<sub>2</sub>Cl<sub>2</sub>)/M06-2X/6-311G(d,p) level of theory. See DOI: 10.1039/b000000x/.

- 1 a) A. Berkessel, in *Organocatalysis by Hydrogen Bonding Networks in Organocatalysis* (Eds.: M. T. Reetz, B. List, H. Jaroach, H. Weinmann), Springer-Verlag Berlin Heidelberg, 2008, Vol 2, pp. 281-297; b) *Hydrogen Bonding in Organic Synthesis* (Ed.: P. M. Pihko), Wiley-VCH, Weinheim, 2009; c) E.-E. Kerstin and A. Berkessel, *Top. Curr. Chem.*, 2010, **291**, 1-27.
- 2 For selected reviews on organocatalysis, see for instance: (a) *Asymmetric Organocatalysis* (Eds.: A. Berkessel, H. Gröger), Wiley-VCH, Weinheim, Germany, 2004; (b) *Acc. Chem. Res.*, 2004, **37** (8), special issue on organocatalysis; (c) *Enantioselective Organocatalysis* (Ed.: P. I. Dalko), Wiley-VCH: Weinheim, Germany, 2007; (d) *Chem. Rev.*, 2007, **107** (12), special issue on organocatalysis; (e) *Recent Developments in Asymmetric Organocatalysis* (Ed.: H. Pellissier), RSC Publishing, Cambridge, 2010; f) *Asymmetric Organocatalysis* (Ed.: B. List) *Top. Curr. Chem.*, 2010, **291**, Springer, Heidelberg; (g) *Curr. Org. Chem.* 2011, **15** (13) special issue on organocatalysis; (h) *Comprehensive Enantioselective Organocatalysis* (Ed.: P. Dalko), Wiley-VCH, Weinheim, 2013.
- 3 For applications of organocatalysis in the synthesis of natural products and non-natural biologically active molecules, see: (a) R. M. de Figueiredo and M. Christmann, *Eur. J. Org. Chem.*, 2007, 2575; (b) E. Marqués-López, R. P. Herrera and M. Christmann, *Nat. Prod. Rep.*, 2010, **27**, 1138; (c) J. Alemán and S. Cabrera, *Chem. Soc. Rev.*, 2013, **42**, 774; (d) E. Marqués-López and R. P. Herrera in *Comprehensive Enantioselective Organocatalysis* (Ed: P. Dalko), Wiley-VCH, Weinheim, 2013, pp 1359-1383.
- 4 (a) P. R. Schreiner, *Chem. Soc. Rev.*, 2003, **32**, 289; (b) Y. Takemoto, *Org. Biomol. Chem.*, 2005, **3**, 4299; (c) S. J. Connon, *Chem. Eur. J.*, 2006, **12**, 5418; (d) M. S. Taylor and E. N. Jacobsen, *Angew. Chem. Int. Ed.*, 2006, **45**, 1520; (e) A. G. Doyle and E. N. Jacobsen, *Chem. Rev.*, 2007, **107**, 5713; (f) H. Miyabe and Y. Takemoto, *Bull. Chem. Soc. Jpn.*, 2008, **81**, 785; (g) Z. Zhang and P. R. Schreiner, *Chem. Soc. Rev.*, 2009, **38**, 1187; (h) E. Marqués-López and R. P. Herrera, *An. Quím.*, 2009, **105**, 5; (i) M. Kotke and P. R. Schreiner, in *Hydrogen Bonding in Organic Synthesis* (Ed.: P. M. Pihko), Wiley-VCH, Weinheim, 2009, pp 141-351; (j) S. J. Connon, *Synlett*, 2009, 354.
- 5 (a) G. Dessole, R. P. Herrera and A. Ricci, *Synlett*, 2004, 2374; (b) R. P. Herrera, V. Sgarzani, L. Bernardi and A. Ricci, *Angew. Chem. Int. Ed.*, 2005, **44**, 6576; (c) D. Pettersen, R. P. Herrera, L. Bernardi, F. Fini, V. Sgarzani, R. Fernández, J. M. Lassaletta and A. Ricci, *Synlett*, 2006, 239; (d) L. Bernardi, F. Fini, R. P. Herrera, A. Ricci and V. Sgarzani, *Tetrahedron*, 2006, **62**, 375; (e) R. P. Herrera, D. Monge, E. Martín-Zamora, R. Fernández and J. M. Lassaletta, *Org. Lett.*, 2007, **9**, 3303; (f) A. Alcaine, E. Marqués-López, P. Merino, T. Tejero and R. P. Herrera, *Org. Biomol. Chem.*, 2011, **9**, 2777; (g) E. Marqués-López, A. Alcaine, T. Tejero and R. P. Herrera, *Eur. J. Org. Chem.*, 2011, 3700; (h) E. Marqués-López and R. P. Herrera in *New Strategies in Chemical Synthesis and Catalysis* (Ed.: B. Pignataro) Wiley-VCH, Weinheim, 2012, pp 175-199; (i) A. Alcaine, E. Marqués-López and R. P. Herrera, *RSC Advances*, 2014, **4**, 9856.
- 6 For reviews on Friedel-Crafts organocatalyzed alkylation reactions, see: (a) E. Marqués-López, A. Diez-Martinez, P. Merino and R. P. Herrera, *Curr. Org. Chem.*, 2009, **13**, 1585; (b) S.-L. You, Q. Cai and M. Zeng, *Chem. Soc. Rev.*, 2009, **38**, 2190; (c) V. Terrasson, R. M. de Figueiredo and J. M. Campagne, *Eur. J. Org. Chem.*, 2010, 2635; (d) M. Zeng and S.-L. You, *Synlett*, 2010, 1289.
- 7 For two pivotal reviews in this area of research, see: (a) A. Berkessel and K. Etzenbach-Effers in *Hydrogen Bonding in Organic Synthesis* (Ed.: P. M. Pihko), Wiley-VCH, Weinheim, 2009, pp 15-42; (b) P. H.-Y. Cheong, C. Y. Legault, J. M. Um, N. Çelebi-Ölçüm and K. N. Houk, *Chem. Rev.*, 2011, **111**, 5042; and references therein cited.
- 8 For selected examples of catalysts containing the aminoindanol moiety, see: (a) D. Almaşi, D. A. Alonso, E. Gómez-Bengoa, Y. Nagel and C. Nájera, *Eur. J. Org. Chem.*, 2007, 2328; (b) M. T. Robak, M. Trincado and J. A. Ellman, *J. Am. Chem. Soc.*, 2007, **129**, 15110; (c) M. Ganesh and D. Seidel, *J. Am. Chem. Soc.*, 2008, **130**,

- 16464; (d) H. Jiang, M. W. Paixão, D. Monge and K. A. Jørgensen, *J. Am. Chem. Soc.*, 2010, **132**, 2775; (e) X.-L. Liu, Z.-J. Wu, X.-L. Du, X.-M. Zhang and W.-C. Yuan, *J. Org. Chem.*, 2011, **76**, 4008; (f) S. S. So, J. A. Burkett and A. E. Mattson, *Org. Lett.*, 2011, **13**, 716.
- 9 L. Simón and J. M. Goodman, *Org. Biomol. Chem.*, 2009, **7**, 483.
- 10 For reviews about thioureas as bifunctional organocatalysts, see: (a) H. Miyabe and Y. Takemoto, *Bull. Chem. Soc. Jpn.*, 2008, **81**, 785; (b) S. J. Connon, *Chem. Commun.*, 2008, 2499.
- 11 For previous studies of the Friedel–Crafts alkylation reaction using phosphoric acid organocatalysts, see: (a) C. Zheng, Y.-F. Sheng, Y.-X. Li and S.-L. You, *Tetrahedron*, 2010, **66**, 2875; (b) T. Hirata and M. Yamanaka, *Chem. Asian J.*, 2011, **6**, 510.
- 12 (a) M. B. Smith and J. March, *March's Advanced Organic Chemistry*, 5th ed.; Wiley, New York, NY, 2000, pp 675-681; For a recent interesting computational study about the C-C bond formation in the Friedel-Crafts alkylation reaction between indole and nitroolefins, see also: (b) L. R. Domingo, P. Pérez and J. A. Sáez, *RSC Advances*, 2013, **3**, 7520.
- 13 For selected computational works involving chiral thiourea catalysts, see: (a) R. Zhu, D. Zhang, J. Wu and C. Liu, *Tetrahedron: Asymmetry*, 2006, **17**, 1611; (b) A. Hamza, G. Schubert, T. Soós and I. Pápai, *J. Am. Chem. Soc.*, 2006, **128**, 13151; (c) S. J. Zuend and E. N. Jacobsen, *J. Am. Chem. Soc.*, 2007, **129**, 15872; (d) E. M. Fleming, C. Quigley, I. Rozas and S. J. Connon, *J. Org. Chem.*, 2008, **73**, 948; (e) C. E. S. Jones, S. M. Turega, M. L. Clarke, D. Philp, *Tetrahedron Lett.* 2008, **49**, 4666; (f) S. J. Zuend and E. N. Jacobsen, *J. Am. Chem. Soc.*, 2009, **131**, 15358; (g) S. Schenker, C. Schneider, S. B. Tsogoeva and T. Clark, *J. Chem. Theory Comput.*, 2011, **7**, 3586; (h) T. E. Shubina, M. Freund, S. Schenker, T. Clark and S. B. Tsogoeva, *Beilstein J. Org. Chem.*, 2012, **8**, 1485; (i) A. Sengupta and R. B. Sunoj, *J. Org. Chem.*, 2012, **77**, 10525; (j) J.-L. Zhu, Y. Zhang, C. Liu, A.-M. Zheng and W. Wang, *J. Org. Chem.*, 2012, **77**, 9813.
- 14 All calculations were carried out with the Gaussian 09 suite of programs: Gaussian 09, Revision A.1, M. J. Frisch, G. W. Trucks, H. B. Schlegel, G. E. Scuseria, M. A. Robb, J. R. Cheeseman, G. Scalmani, V. Barone, B. Mennucci, G. A. Petersson, H. Nakatsuji, M. Caricato, X. Li, H. P. Hratchian, A. F. Izmaylov, J. Bloino, G. Zheng, J. L. Sonnenberg, M. Hada, M. Ehara, K. Toyota, R. Fukuda, J. Hasegawa, M. Ishida, T. Nakajima, Y. Honda, O. Kitao, H. Nakai, T. Vreven, Jr., J. A. Montgomery, J. E. Peralta, F. Ogliaro, M. Bearpark, J. J. Heyd, E. Brothers, K. N. Kudin, V. N. Staroverov, R. Kobayashi, J. Normand, K. Raghavachari, A. Rendell, J. C. Burant, S. S. Iyengar, J. Tomasi, M. Cossi, N. Rega, N. J. Millam, M. Klene, J. E. Knox, J. B. Cross, V. Bakken, C. Adamo, J. Jaramillo, R. Gomperts, R. E. Stratmann, O. Yazyev, A. J. Austin, R. Cammi, C. Pomelli, J. W. Ochterski, R. L. Martin, K. Morokuma, V. G. Zakrzewski, G. A. Voth, P. Salvador, J. J. Dannenberg, S. Dapprich, A. D. Daniels, Ö. Farkas, J. B. Foresman, J. V. Ortiz, J. Cioslowski, D. J. Fox, Gaussian, Inc., Wallingford CT, 2009.
- 15 CCDC-976490 (**4ba**) contains the supplementary crystallographic data for this paper. These data can be obtained free of charge from the Cambridge Crystallographic Data Centre via [www.ccdc.cam.ac.uk/data\\_request/cif](http://www.ccdc.cam.ac.uk/data_request/cif).
- 16 (a) M. C. Etter and T. W. Panunto, *J. Am. Chem. Soc.*, 1988, **110**, 5896; (b) M. C. Etter, Z. Urbańczyk-Lipkowska, M. Zia-Ebrahimi and T. W. Panunto, *J. Am. Chem. Soc.*, 1990, **112**, 8415; (c) M. C. Etter, *Acc. Chem. Res.*, 1990, **23**, 120; (d) T. R. Kelly and M. H. Kim, *J. Am. Chem. Soc.*, 1994, **116**, 7072.
- 17 D. A. Yalalov, S. B. Tsogoeva and S. Schmatz, *Adv. Synth. Catal.*, 2006, **348**, 826.
- 18 M. P. Sibi and K. Itoh, *J. Am. Chem. Soc.*, 2007, **129**, 8064.
- 19 Y. Zhao and D. G. Truhlar, *Acc. Chem. Res.*, 2008, **41**, 157.
- 20 (a) A. D. McLean and G. S. Chandler, *J. Chem. Phys.*, 1980, **72**, 5639; (b) K. Raghavachari, J. S. Binkley, R. Seeger and J. A. Pople, *J. Chem. Phys.*, 1980, **72**, 650.
- 21 K. Fukui, *Acc. Chem. Res.*, 1981, **14**, 363.